Dislocation Structure in a Single-Crystal Nickel-Base Superalloy during Low Cycle Fatigue

J.H. ZHANG, Z.Q. HU, Y.B. XU, and Z.G. WANG

An investigation of dislocation structure in a single crystal nickel-base superalloy during low cycle fatigue (LCF) at 760 °C has been conducted. Dislocation bands are found to be produced first in the matrix in some defined directions. With an increase in cycle numbers, there is an increase in dislocation density in the bands and a decrease in the spacing between the bands, leading to the formation of the dislocation walls or cells. Sometimes, three-dimensional (3-D) networks are formed also by the interaction between two sets of parallel dislocations. The Burgers vectors of the dislocations in the network are 1/2 ⟨110⟩. Clustering of dislocations eventually occurs at γ'/γ interfaces because of the obstruction of the γ'-particles to moving dislocations. Most of the dislocations observed in the γ'-phases are in the form of superdislocations. Dislocation shearing through the γ'-phase was found occasionally. Reprecipitation of γ'-phase induced by strain was also observed in the present study.

I. INTRODUCTION

NICKEL-base superalloy undergoes two processes during cycling: the strain hardening and softening and the nucleation and propagation of a microcrack. The cyclic hardening and then softening occur over the whole deformation process. However, the nucleation and propagation of microcrack are superposed in the later stage of the hardening and softening processes. Although every event, which is very complex, within the process is affected by the microstructure, the mechanism of the process is related to the creation, motion, and reaction of dislocations. A number of experimental and theoretical investigations on the dislocation structure in the nickel-base superalloy and ordered materials have been conducted.[1-5] However, few works on dislocation structure produced during low cycle fatigue (LCF) in the single-crystal nickel-base superalloy have been reported in detail. As part of a series of an extensive study, in this article, the emphasis will be put on the behavior of dislocations produced during LCF in a single-crystal nickel-base superalloy.

II. MATERIALS AND PROCEDURES

The single-crystal nickel-base superalloy used in this investigation had a composition of (in wt pct) 15Cr, 8.40Co, 5.85W, 3.91Al, 3.98Ti, 1.03Ta, and balance Ni. The alloy was heat-treated as follows: 1100 °C/8 h AC + 1240 °C/4 h AC + 1090 °C/2 h AC + 850 °C/24 h AC.

Low cycle fatigue tests at 760 °C were carried out after the heat treatment. A full reversed triangular wave with a frequency range of 15 to 25 cycles per minute has been used. The stress ratio (R) is -1, the stress amplitude range is from 550 to 800 MPa, and the stress axis is parallel to the crystal growth direction [001].

J.H. ZHANG and Y.B. XU, Associate Professors, and Z.Q. HU and Z.G. WANG, Professors, are with the State Key Laboratory for Fatigue and Fracture of Materials, Institute of Metal Research, Chinese Academy of Sciences, Shenyang 110015, People's Republic of China.

Manuscript submitted April 2, 1991.

The thin foils for observation by transmission electron microscopy (TEM) have been prepared by the twin jet polishing method. Dislocation structure has been examined in a PHILIPS* EM 420 microscope using a double tilt goniometer in diffraction and imaging modes.

*PHILIPS is a trademark of Philips Electronic Instruments Corp., Mahwah, NJ.

III. EXPERIMENTAL RESULTS

A. *Initial Structure of the Alloy*

As shown in Figure 1, the microstructure in the heat-treated condition is composed of γ matrix and cuboidal γ'-precipitates which are completely coherent with the matrix. The misfit ($\delta = 2(a_{\gamma'} - a_\gamma)/a_{\gamma'} + a_\gamma$) is 0.05 pct.[6] The weight fraction of γ'-phase with average size of 250 nm in the alloy is 52.4 pct.

B. *S-N Curve*

The relationship between applied stress and life to failure is shown in Figure 2, where the markers 16, 5, 10, 12, and 13 correspond to those at which the foil specimens for TEM examination were prepared.

C. *Dislocation Structure in Matrix*

Transmission electron microscopy observation reveals that strain distribution in LCF specimens is quite inhomogeneous, and dislocations are found to be generated in the matrix between γ' particles preferentially and to form dislocation bands. These can be seen clearly in Figure 3, which shows dislocation bands produced during LCF at 800 MPa for 2763 cycles. Contrast analysis shows that the orientation of the dislocation bands approaches [00$\bar{1}$] (Figure 3(a)). However, the orientations of the intersecting dislocation bands in Figure 3(b) are near [00$\bar{1}$] and [211]. There are a few singly activated dislocations in between the bands. When the stress amplitude is 650 MPa and the cyclic number is increased to 7981, walls of dislocations are found to be formed in the alloy matrix, as shown in Figures 4(a) and (b). The

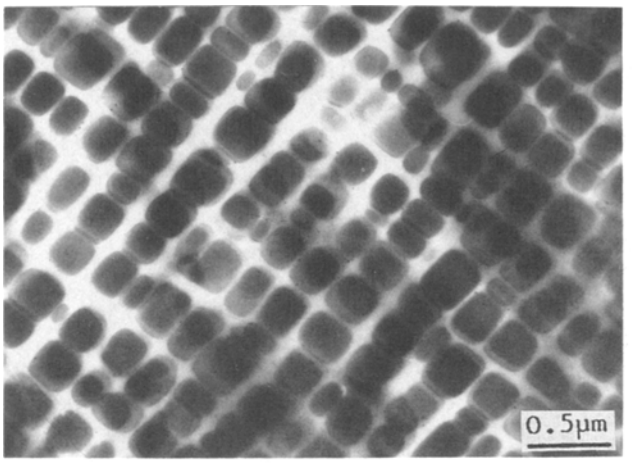

Fig. 1 — Microstructure of the alloy after heat treatment.

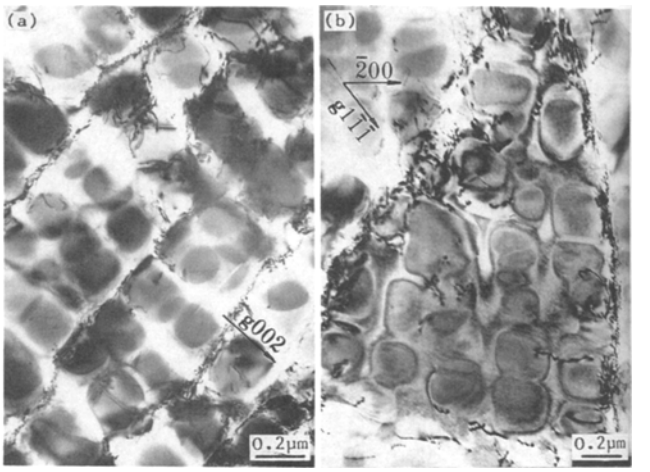

Fig. 4 — Dislocation (*a*) wall and (*b*) cells in matrix.

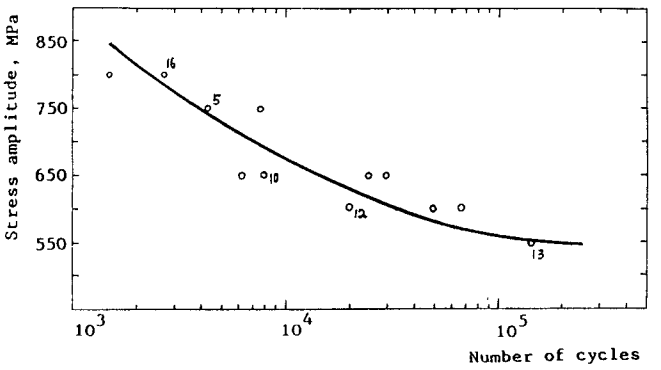

Fig. 2 — Variation of stress amplitude as a function of the cyclic number of the alloy fatigued at 760 °C.

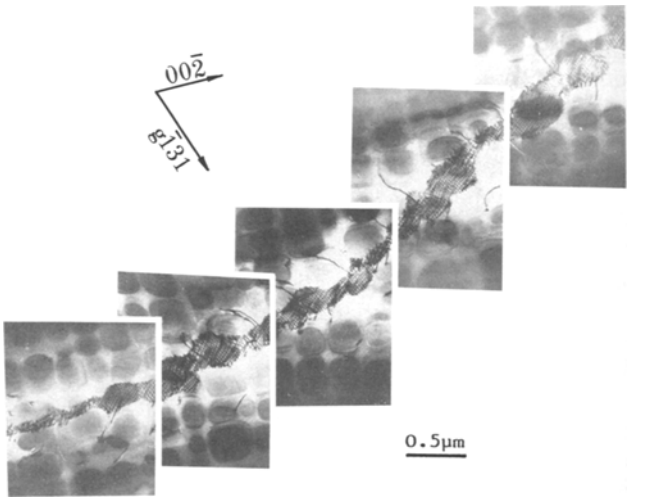

Fig. 5 — Dislocation networks in matrix.

orientation of the dislocation walls is along the [010] direction (Figure 4(a)). Sometimes the walls are configured to form triangular cells (Figure 4(b)).

The directions of the right-angled sides are near [001] and [010], and the inclined one approaches [121]. We

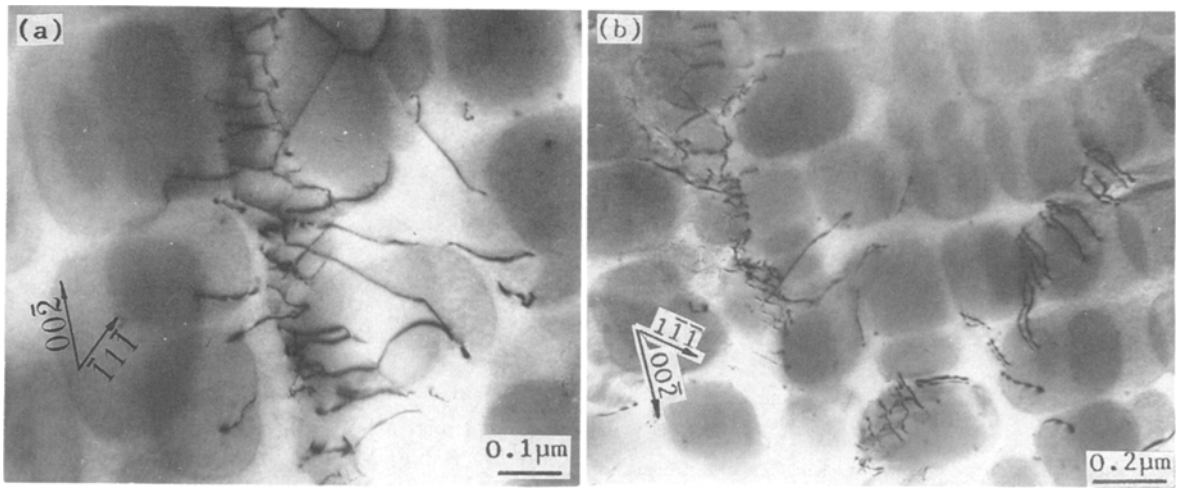

Fig. 3 — TEM micrographs showing the dislocation in (*a*) a single band and (*b*) in twin bands.

believe these bands and walls of dislocations are formed by moving dislocations being absorbed gradually.

Another prominent feature of the dislocation structure in the present study is the formation of a three-dimensional (3-D) network of dislocations under LCF at 800 MPa for 2763 cycles, as shown in Figure 5.

The dislocation networks have been developed by absorbing moving dislocations crossing a few tens of γ'-precipitates. In order to understand the formation mechanism and the nature of the dislocation networks, the Burgers vectors of dislocations have been determined in detail by using the invisibility criterion in a transmission electron microscope with twin tilt goniometer stage, as shown in Figures 6(a) through (3d). Figure 6(a) shows triple dislocation net, where $\mathbf{b}_1$, $\mathbf{b}_2$, and $\mathbf{b}_3$ represent the Burgers vectors and directions of the three kinds of

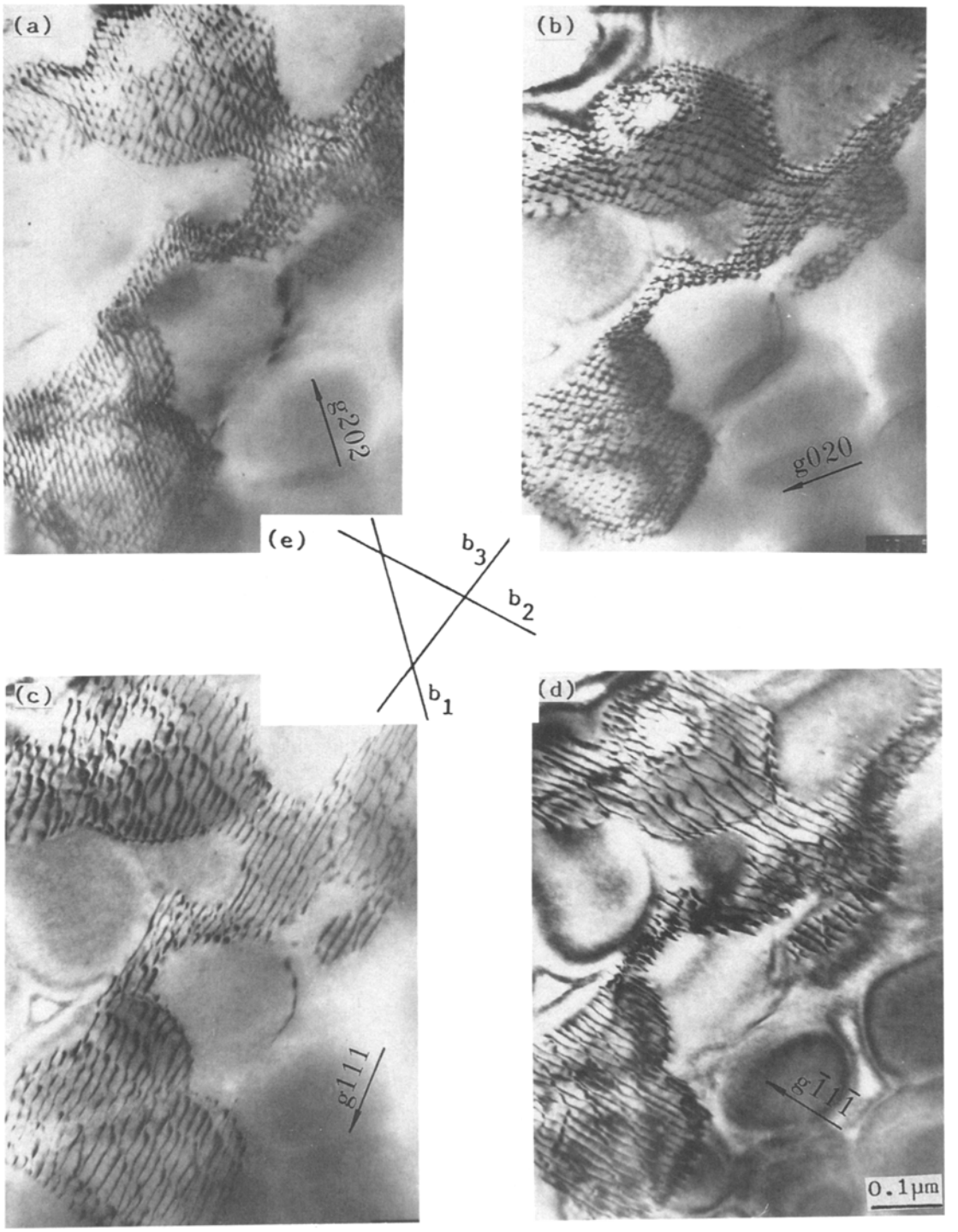

Fig. 6—(*a*) 3-D networks of dislocation in matrix and (*e*) directions of dislocation lines in three sets. (*b*) The dislocations were invisible in the $\mathbf{b}_1$ set when $\mathbf{g}_1(020)$ and $\mathbf{g}_2(\bar{2}02)$ were used to image. Similarly, the dislocations in (*c*) $\mathbf{b}_2$ and (*d*) $\mathbf{b}_3$ were invisible when $\mathbf{g}_3(111)$ and $\mathbf{g}_4(200)$ and $\mathbf{g}_5(\bar{1}1\bar{1})$ and $\mathbf{g}_6(2\bar{2}0)$, respectively, were used to image.

dislocations (Figure 6(e)). When $\mathbf{g}_1(020)$ and $\mathbf{g}_2(\bar{2}02)$ diffraction conditions have been used to form images under two-beam condition, the dislocations in the $\mathbf{b}_1$ set are invisible, as shown in Figure 6(b). Therefore, the Burgers vector in the $\mathbf{b}_1$ set is $1/2[101]$. Similarly, $\mathbf{b}_2 = 1/2[01\bar{1}]$ and $\mathbf{b}_3 = 1/2[110]$ when diffraction vectors $\mathbf{g}_3(111)$ (Figure 6(c)) and $\mathbf{g}_4(200)$ and $\mathbf{g}_5(\bar{1}1\bar{1})$ (Figure 6(d)) and $\mathbf{g}_6(2\bar{2}0)$, respectively, are used to form images. The direction of dislocation lines in the $\mathbf{b}_1$ set is parallel to its Burgers vector, indicating that the dislocations in the $\mathbf{b}_1$ set are of the screw type. The dislocations in the other two sets are of the screw type also.

D. *Interaction of Dislocations with the Ordered γ′-Phase*

In general, there are a large number of dislocations in the matrix in deformed specimens of the single-crystal nickel-base superalloy. However, superdislocations were found to be formed in the γ′-phase after the specimen was deformed to a large number of cycles. For example, Figures 7(a) and (b) show the clustering of dislocations in the matrix and the formation of an antiphase domain (APD) (indicated by arrow), respectively, during LCF under 550 MPa for 143,774 cycles. Analysis shows that the Burgers vectors of the superpartial dislocations associated with the APD stacking faults with the displacement $1/2[110]$ are $1/2\langle 110\rangle$. The dislocations shearing through γ′-particles were also found, as shown in Figure 8, indicating the formation of a slip channel of dislocations in the γ′-phase. The slip direction of the dislocations is [112]. This kind of slip appears here only to shear over one γ′-particle because of the obstacle of the next γ′-particle against the dislocations.

It is fascinating to note that the strain induces a phase transformation in the specimen fatigued at 750 MPa for 4458 cycles, as shown in Figure 9(a), where a large number of fine globular γ′-precipitates were formed in the alloy matrix. It was found that these fine globular particles are efficient obstacles against the movement of dislocations in the matrix. This observation is similar to those of Wang *et al.*[7] and Laird *et al.*[8] They found that the cyclic strain induced the change of carbide in morphology in Cr-Mo-V steel and the formation of

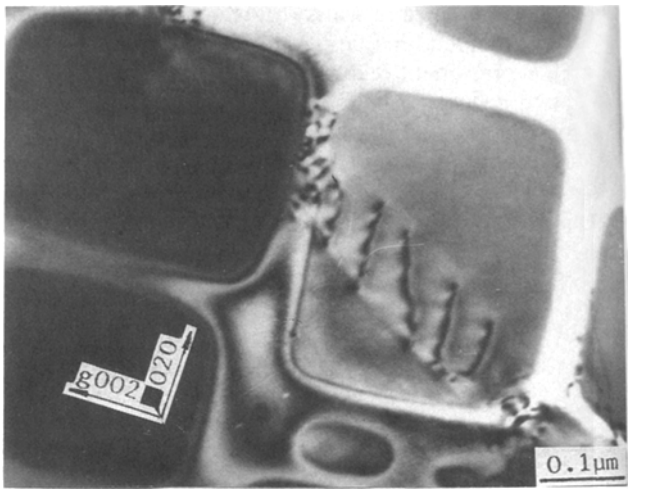

Fig. 8—Dislocations passing through the γ′-phase.

γ′-platelets in the precipitation-hardened Al-15 wt pct Ag alloy. It was also found that the cuboid γ′-particles were frequently sheared by dislocations (Figure 9(b)). It would be expected that this phenomenon is surely considered to be associated with the reprecipitation of the fine globular γ′-phase in the matrix. However, further work is needed to understand why the reprecipitation of the γ-phase induced by strain can occur in this situation.

For the specimens deformed cyclically at 550-MPa for 143,774 cycles, an equilibrium distribution of dislocations was found to appear in the fully deformed region. The matrix is filled with tangled dislocations. Antiphase domains were observed in most of the γ′-particles (Figure 10(a)). The traces of the antiphase boundaries (APB) with the foil planes are all parallel to $[0\bar{1}1]$. The cooperative deformation of the matrix with γ′-precipitates was also found in the same observed region. This is shown in Figure 10(b), where dislocation networks roughly align along the direction 45 deg to the stress axis and the orientation of the APBs is parallel to the same direction also.

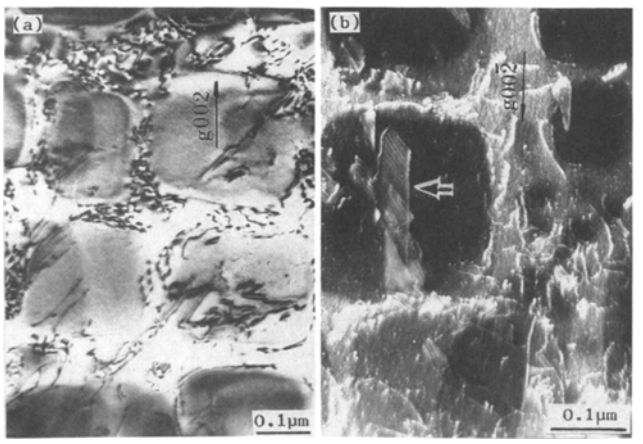

Fig. 7—Pileup of (*a*) dislocations in matrix and (*b*) superdislocations in γ′-phase (weak-beam imaging).

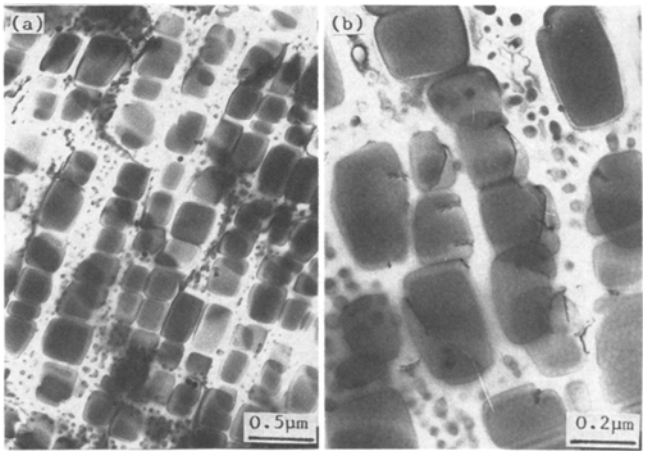

Fig. 9—(*a*) Reprecipitation of γ′-phases induced by strain and (*b*) dislocations cut through the cuboid particles.

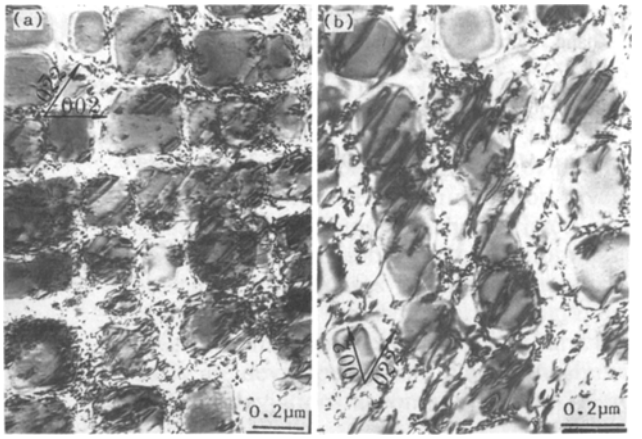

Fig. 10—(*a*) Dislocation networks in matrix and APB in γ'-phase and (*b*) cooperative deformation of matrix with γ'-phase.

IV. DISCUSSION

A. *Formation Mechanism of Dislocation Network in Matrix*

As shown in Figures 5 and 6, 3-D dislocation networks produced under cyclic deformation are considered to result from the reaction of two sets of parallel dislocations arising from the misfit interface between the matrix and γ'-precipitates. Figure 11(a) shows schematically this kind of reaction between dislocations, which can be expressed as follows:

$$\mathbf{b}_1 + \mathbf{b}_2 \rightarrow \mathbf{b}_3$$

where $\mathbf{b}_1$ and $\mathbf{b}_2$ represent the Burgers vectors of dislocations in two sets and $\mathbf{b}_3$ is the Burgers vector of the combination dislocation. The result can be given by

$$1/2[101] + 1/2[01\bar{1}] \rightarrow 1/2[110]$$

Because of the line tension, the dislocations reduce their lengths until the equilibrium state is reached (Figure 11(b)). Due to the inhomogeneous stress on the dislocations and the different observed directions, the final dislocation networks develop, as shown in Figure 6(a).

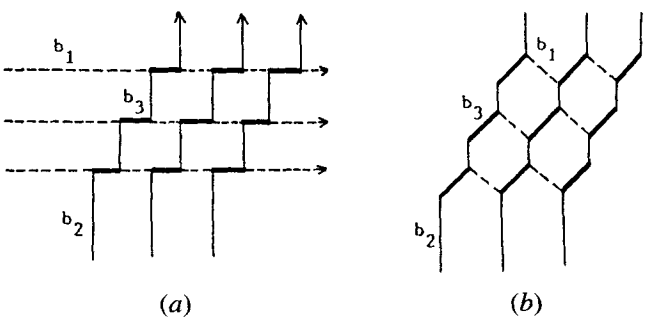

Fig. 11—(*a*) Reaction in two-set parallel dislocations and (*b*) the formation of a dislocation network.

B. *The Change in Dislocation Structure in LCF*

The first structure observed in this alloy during LCF at 760 °C is the formation of dislocation bands at a defined orientation. As the cyclic number is increased, the dislocation density in the bands is increased and the spacing between the bands is decreased. These processes lead to the formation of dislocation walls or cells which cause the fatigue hardening of the alloy. However, the avalanche of dislocation walls or cells and the compatible deformation of the matrix with γ'-phase are responsible for the occurrence of the softening of the alloy.

It is evident that the γ'-phase can efficiently suppress the glide of dislocations over a long distance and enhance the fatigue strength. These are considered to arise from the suitable size and the small misfit of γ'-phase with the matrix. In addition, a large number of APB in the γ'-phase can also lead to further strengthening of the alloy.

V. SUMMARY AND CONCLUSIONS

1. During the LCF of the alloy at 760 °C, dislocation bands are formed in the matrix at defined orientations. The dislocation density in the bands is increased and the spacing between the bands is decreased with the increase of cyclic numbers. These lead to the formation of dislocation walls or cells.
2. Another feature of dislocation structures produced in LCF is the formation of a 3-D network of dislocations in the matrix. These networks are caused by the reactions between two-set parallel dislocations. These dislocations have the Burgers vector $1/2\langle 110\rangle$ which is the smallest perfect atomic displacement in the matrix.
3. Because of the γ'-phase, the dislocations initially do not glide over a long distance in the matrix. Most of the dislocations in the γ'-phase are in the form of superdislocations.
4. During the process of fatigue softening, the dislocation structure in both matrix and γ'-phase is characterized by compatible deformation.
5. Reprecipitation of γ'-phase induced by strain was observed during cyclic deformation under 750 MPa at 760 °C.

ACKNOWLEDGMENTS

This study was supported by the National Natural Science Foundation of China. The authors wish to thank Mr. Z.Y. Zhang, Y.J. Tang, and Y.A. Li for preparing the samples.

REFERENCES

1. Wen Mao and Lin Dongliang: *Acta Metall. Sin.*, 1990, vol. 3A, pp. 79-88.
2. P. Lours, A. Coujou, and B. DeMauduit: *Phil. Mag.*, 1990, vol. A62, pp. 253-66.
3. F.D. Tichelaar and F.W. Schapink: *Phil. Mag.*, 1990, vol. A62, pp. 53-76.

4. M. Dollar and I.M. Bernstein: in *Superalloys 1988*, Proc. of the Sixth Int. Symp. on Superalloys, D.N. Duhl, G. Maurer, S. Antolovich, C. Lund, and S. Reichman, eds., TMS-AIME, Warrendale, PA, 1988, pp. 275-84.
5. T.M. Pollock and A.S. Argon: in *Superalloys 1988*, Proc. of the Sixth Int. Symp. on Superalloys, D.N. Duhl, G. Maurer, S. Antolovich, C. Lund, and S. Reichman, eds., TMS-AIME, Warrendale, PA, 1988, pp. 285-94.
6. Zhang Jinghua, Tang Yajun, and Hu Zhuang qi: *Mater. Sci. Prog.*, 1990, vol. 4, pp. 392-97 (in Chinese).
7. Z.G. Wang, K. Pahka, and C. Laird: *Acta Metall.*, 1985, vol. 33, pp. 2129-42.
8. C. Larid, V.J. Langelo, M. Hollrah, N.C. Yang, and R. Dela Veaux: *Mater. Sci. Eng.*, 1978, vol. 32, pp. 137-60.